Communication

New algorithm for QT interval analysis in 24-hour Holter ECG: performance and applications

P. Laguna[1] N. V. Thakor[2] P. Caminal[1] R. Jané[1] Hyung-Ro Yoon[2]

with the collaboration of

A. Bayés de Luna[3] V. Martí[3] Josep Guindo[3]

[1]Instituto de Cibernética, Universitat Politècnica de Catalunya—CSIC, Avenida Diagonal, 647, planta 2, 08028 Barcelona, Spain
[2]Department of Biomedical Engineering, The Johns Hopkins University, School of Medicine, Baltimore, MD 21205, USA
[3]Servicio de Cardiologia y Unidad Coronaria, Hospital de la Santa Creu i Sant. Pau., Universidad Autonoma de Barcelona, Sant Antonio M. Claret 167, 08025 Barcelona, Spain

Keywords—*Algorithm, ECG, Holter recordings, Patient monitoring, QRST complexes*

Med. & Biol. Eng. & Comput., 1990, 28, 67–73

1 Introduction

CARDIOVASCULAR DISEASES are the primary cause of death in the adult population. Half of cardiac deaths occur as sudden death. Many studies have been performed in recent years to show the relationship between QT interval and prognosis in postmyocardial infarction patients (PMIPs) (PUDDU *et al.*, 1981; PUDDU and BOURASSA, 1986; SCHWARTZ and WOLF, 1978; AHNVE *et al.*, 1978; TAYLOR *et al.*, 1981). An abnormal QTc (QT corrected with Bazett's formula (BAZETT, 1920)) prolongation in surface can be associated with serious ventricular arrhythmias, syncope and sudden death. We have also demonstrated that the dynamic behaviour of QT measurements made by hand in Holter tapes could be a marker of malignant ventricular arrythmias (MVAs) (MARTÍ *et al.*, 1988). Thus QT interval measurement in Holter tapes assumes great importance in diagnostic ECG, and several methods are proposed in the literature to implement QT measurement, trying to solve the problem of detecting QRS-wave beginning and T-wave end (ALGRA *et al.*, 1987; PISANI *et al.*, 1985; CRITELLI *et al.*, 1982). The most difficult problem is to define the T-wave end, because of its low frequency components. Some criteria for T-wave end definition (ALGRA *et al.*, 1987; CRITELLI *et al.*, 1982) are based on deflection with reference to the baseline, whereas others make use of first derivative and some threshold (PISANI *et al.*, 1985).

We present a new algorithm which makes use of the first derivative and morphology of each T-wave, and compare its performance with that of manual measurements on a set of approximately 40 beats at the beginning of 18 selected Holter tapes. As an example we present the results obtained from a 24-hour Holter ECG signal.

2 Methods

We analysed the data (lead II) recorded on a Holter system (ICR-6500) with a frequency response of 0·05–100 Hz (−3 dB). Holter tapes were played back on a DR tape recorder (Teac model R-61). Analogue signals were digitised using a 12-bit resolution data-acquisition system installed on a Compaq Model III computer, at an equivalent sampling rate of 250 samples s^{-1}. Data were stored in the computer for subsequent detailed analysis. We have developed a new algorithm which is composed of several steps: preprocessing, QRS detection to position beats, QRS onset and T-wave end definition, and selection of possible noisy beats in order to remove them.

2.1 *Algorithm*

2.1.1 *Preprocessing:* In a first step we use a low-pass differentiator (LPD) for QRS detection with the following transfer function

$$G_1(z) = 1 - Z^{-6} \tag{1a}$$

The amplitude response is

$$|G_1(\omega T)| = 2|\sin(3\omega T)| \tag{1b}$$

where T is the sampling period, gain is $6T$, and the filter processing delay is three samples. We will refer to $d(k)$ as the differentiated ECG signal.

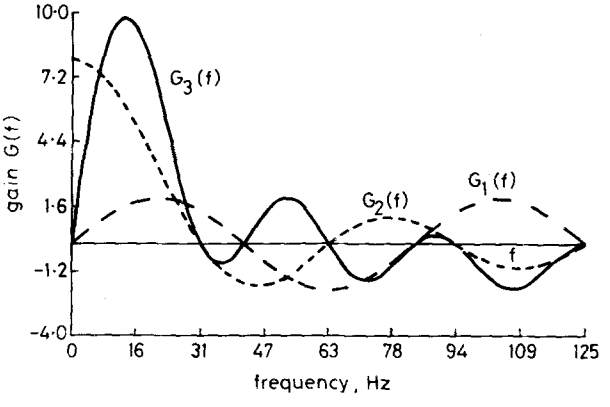

Fig. 1 *Transfer functions for differentiator filter $G_1(f)$, low-pass filter $G_2(f)$ and combination of both $G_3(f)$*

First received 26th October 1988 and in final form 17th May 1989

After that we filter the signal with a first-order low-pass filter to avoid residual noise and intrinsic differentiation noise. LYNN (1977) suggested the transfer function of such an integer coefficient filter:

$$G_2(z) = \frac{1 - Z^{-8}}{1 - Z^{-1}} \tag{2a}$$

The amplitude response is

$$|G_2(\omega T)| = \left| \frac{\sin(4\omega T}{\sin(1/2\omega T)} \right| \tag{2b}$$

DC gain is 8, cutoff frequency at -3 dB is about 20 Hz, and filter delay is $4\frac{1}{2}$ samples. Fig. 1 shows transfer functions for the differentiator $G_1(f)$, low-pass filter $G_2(f)$ and the combination of both $G_3(f) = G_1(f)G_2(f)$.

In future references we will refer to the processed signal $f(k)$ as the differentiated plus low-pass filtered signal.

2.1.2 *QRS detection:* Once the signal is differentiated and filtered, we implement a QRS detector based on an adaptive threshold as described in PAN and TOMPKINS (1985), with some modifications to increase processing speed and make Q and R-wave peak definition easier.

We define a threshold at the n beat as H_n and we detect QRS as the first maximum or minimum whose absolute value is larger than H_n. As a first step we look for the highest positive or negative peak in the first 2 s signal, and define PK_1 as the absolute value of this initial peak. Then we make $H_1 = 0{\cdot}8PK_1$ (80 per cent of peak value).

If PK_n denotes the maximum absolute value of the QRS at the n beat in the processed signal, we calculate the next threshold H_{n+1} as

$$H_{n+1} = 0{\cdot}8H_n + 0{\cdot}2(0{\cdot}8PK_n) \tag{3}$$

We also implement a recursive search back for missing beats, with a lower threshold $H'_n(H'_n = 4/5H_n)$, as in PAN and TOMPKINS (1985), when the next beat is farther than 1·8 times the current R–R interval average (RR_{av}). We also calculate the actual RR_{av} from the last R–R interval (RR)

$$RR_{av} = \begin{cases} 0{\cdot}8RR_{av} + 0{\cdot}2RR & 1{\cdot}5RR_{av} > RR > 0{\cdot}5RR_{av} \\ RR_{av} & \text{otherwise} \end{cases} \tag{4}$$

2.1.3 *R and Q-waves definition:* After detecting the PK_n position in the processed signal $f(k)$, we search for the nearest peak forward (PK_a, peak after) and backwards (PK_b, peak before) as described in Fig. 2. To define the R-position R_p: we know that the R-wave has the highest slope in the QRS complex; thus PK_n will be the maximum slope value on either the upward-going side or downward-going side of the R-wave. The other highest slope side of the R-wave will be either PK_a or PK_b, depending which has the larger absolute value. Then we define the R-position R_p as the zero-crossing between PK_n and the highest absolute value of PK_a or PK_b. Fig. 3 shows the flowchart of this algorithm.

In some QRS morphologies the Q or S-wave can be consistently detected as the R-wave. As we are interested in the R–R interval and in normal beats the Q–Q, R–R, or S–S intervals have the same value, we do not take this into consideration.

We define the Q-position Q_p as the zero-crossing preceding the R_p position in the differentiated signal (Fig. 2), and not in the filtered ECG, because the Q-wave has high frequencies that cannot be present in a low-pass filtered signal. When the $R_p - Q_p$ interval exceeds 80 ms no Q-wave is considered. This occurs when the Q-wave has been detected as an R-wave or when no Q-wave is present.

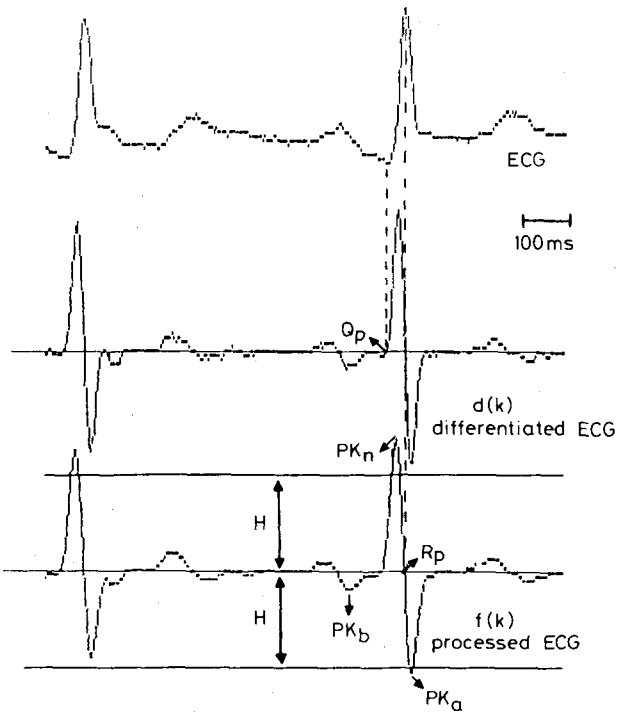

Fig. 2 *Original ECG played back from a Holter tape, output signal of the differentiated preprocessing (differentiated ECG) and output of the low-pass filter after differentiation (processed ECG). The threshold H for QRS detection and PK_n, PK_a, PK_b, R_p and Q_p positions are shown as described in text*

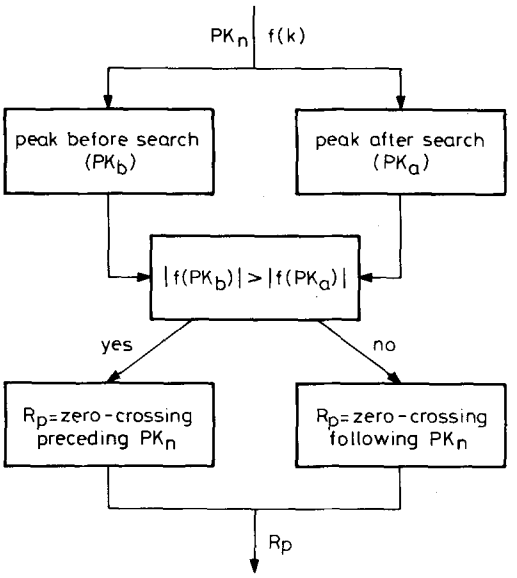

Fig. 3 *Flowchart for R-wave position definition R_p, where the inputs are PK_n (detected peak) and $f(k)$ (processed signal)*

2.1.4 *QRS onset definition:* In the next stage we define QRS onset (QRS_1) as the beginning of the Q-wave (or R-wave when no Q-wave is present). The Q-position Q_p and the R-position R_p have already been detected. Then from the Q_p (or R_p) point we search backwards, in the differentiated signal $d(k)$, for a point Q_i (or R_i) of maximum slope in the ECG signal (Fig. 4). With this point we define a threshold H_q (or H_r) as the value of the differentiated signal in Q_i (or R_i) divided by a constant K which takes the value $K = K_q$ when the Q-wave is present, and $K = K_r$ when no Q-wave is present; $H_q = d(Q_i)/K_q$ (or $H_r = d(R_i)/K_r$). From this point we define QRS-begin (QRS_1) as the backwards threshold crossing point from Q_i (or R_i). The flow chart for this implementation is also shown in Fig. 5. The algorithm performs best for $K_q = 2$ and $K_r = 5$.

We used different K-values in the case of Q-wave presence (K_q) or only R-wave (K_r) due to different maximum slope value for both waves. That considers the R-wave beginning at a position where the slope value reaches $\frac{1}{5}$ ($K = 5$) of the maximum, and $K = 2$ for the Q beginning.

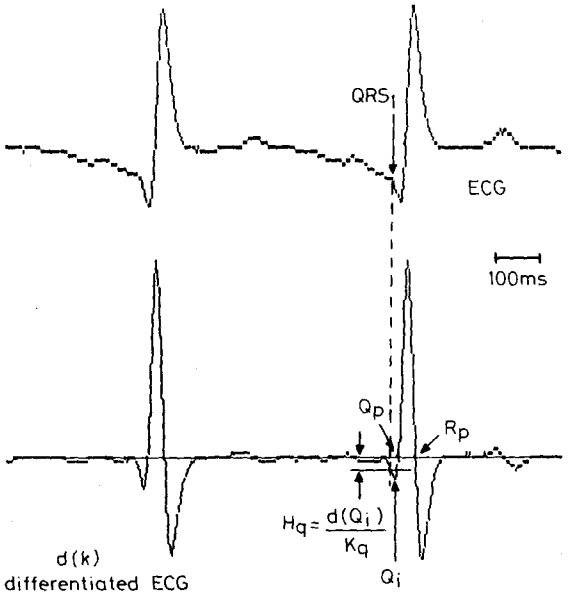

Fig. 4 *Original ECG and differentiated ECG where the QRS onset (QRS_1) point definition is shown, with the Q-position Q_p, the point of maximum slope Q_i and H_q threshold value*

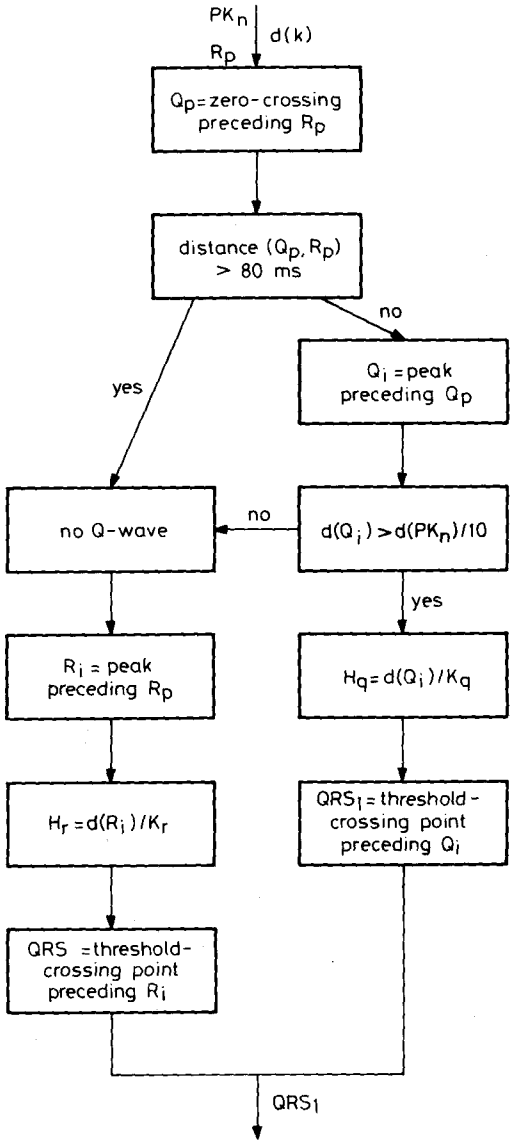

Fig. 5 *Flowchart for QRS onset definition QRS_1, where the inputs are PK_n, R_p, and $d(k)$ (differentiated signal)*

2.1.5 *T-wave peak and T-wave end definition:* From the R-position we define a search window whose limits are *bwind* and *ewind* (Fig. 6).

$$(bwind,\ ewind) = \begin{cases} (140,\ 500)\,\text{ms} & RR_{av} > 700\,\text{ms} \\ (100,\ 0{\cdot}7RR_{av})\,\text{ms} & RR_{av} < 700\,\text{ms} \end{cases} \quad (5)$$

We decrease the window size when R–R decreases, to avoid the next P-wave being detected as a false T-wave. RR_{av} is used to avoid strong changes in the R–R interval. Four different kinds of T-waves are going to be considered: normal T-wave (upward-downward), inverted T-wave (downward-upward), only-downward T-wave, and only-upward T-wave.

We search for the maximum (*max*) and minimum (*min*) values of the processed signal $f(k)$ in the defined window, as shown in Fig. 6. If the *max* position is before the *min* position, then the T-wave may be upward-downward or only upward; $|max| > 4|min|$ is the selected condition to characterise the only-upward T-wave.

If the *min* position is before the *max* position we search for the minimum (*mina*) between the *max* position and the end of the window. If *mina* is comparable in absolute value with *max* we consider again the upward-downward shape. If not, we compare *min* and *max*, and if they have similar values, T downward-upward is considered, otherwise T only-downward is assumed. We have obtained a good performance for classification of the four defined T-wave morphologies using a factor of four for the comparison of *mina* with *max*, and *min* with *max*.

if $|max| < 4|mina|$, then normal T, otherwise next criterion
if $|min| > 4|max|$, then only-downward T-wave, otherwise T-wave inverted

With these considerations we have the last highest slope point of the T-wave (downward or upward), and from this point T_i we search for the T-end point as follows.

Let $f(T_i)$ denote the value of the processed signal at this point (sometimes it will be *min*, *max* or *mina* depending on the T-wave morphology). This value has information on the T-decay rate. We define the T-wave end point T_2 as a forward point from T_i where the downward (or upward in T-inverted) processed signal reaches a threshold value H_t; $H_t = f(T_i)/K_t$, where K_t is an experimental value that in our study has its best performance for $K_t = 2$.

This is the most important step of the algorithm. Note that other methods make use of a differentiated signal (PISANI *et al.*, 1985) and a threshold that has no information on the T-decay rate. In our case, when the T-wave has a higher or lower slope value, $f(T_i)/K_t$ also has a higher or lower value to reach the T-end point. Low-frequency baseline interferences have great importance in methods for T-wave end definition based on baseline considerations (ALGRA *et al.*, 1987; CRITELLI *et al.*, 1982). In our method these have poor influence, because these baseline interferences are of lower frequency than those of the T-wave, and the differentiator has very poor gain for these frequencies in comparison with its gain for T-wave frequencies.

The T-wave peak T_1 is now defined as the first zero-crossing backwards from the T_i position in the processed signal. Fig. 7 shows a flowchart for this procedure.

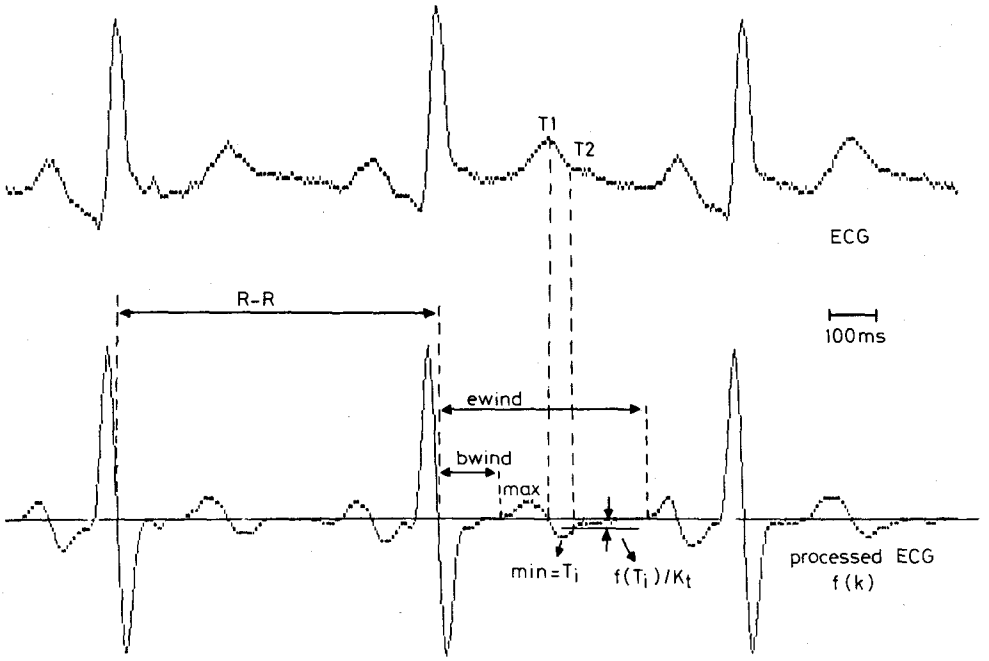

Fig. 6 *Original ECG and processed ECG. In the processed signal the T-end definition algorithm is described where bwind is the distance from the R-position to the beginning of the search window, ewind is the distance from the R-position to the end of this window, max and min are maximum and minimum positions of the processed signal in this window, and $f(T_i)/K$ is the threshold for the T-end wave search. Broken lines indicate R-positions, window limits and correspondence with the T-wave peak T_1 and T-wave end T_2 in the original signal*

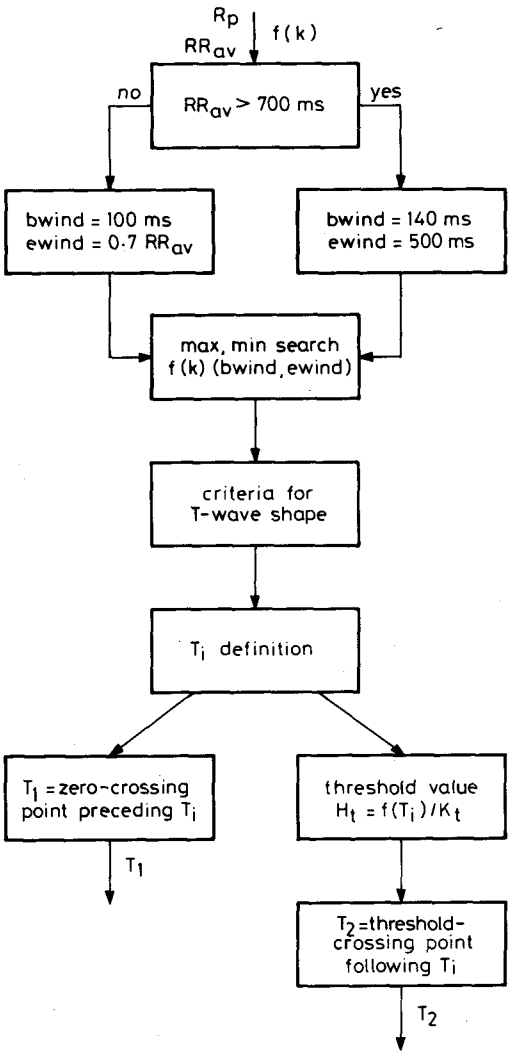

Fig. 7 *Flowchart for T-wave peak T_1, and T-wave end T_2 definition, where inputs are R_p, $f(k)$ and RR_{av} (current R–R interval average)*

2.2 *QT values selection*

Once the QRS onset (QRS_1), T-wave peak T_1 and T-wave end T_2 have been defined, we can calculate the QT interval by subtracting the QRS_1 time from T_2. We also define QTP as an interval between the beginning of the QRS-wave and the T-wave peak (CRITELLI *et al.*, 1982). Finally, we can apply Bazett's formula to obtain the QT and QTP-intervals corrected for R–R interval variability: QT_c and QTP_c, respectively.

$$QT = T_2 - QRS_1 \qquad QT_c = \frac{QT}{\sqrt{RR}} \tag{6a}$$

$$QTP = T_1 - QRS_1 \qquad QTP_c = \frac{QTP}{\sqrt{RR}} \tag{6b}$$

where RR is the previous R–R interval.

As ECGs from Holter tapes unfortunately have an important high-frequency noise contamination, errors can occur in QT-interval definition, due fundamentally to changes in the end of the T-wave leading to wrong T-end definition. Also ectopic and other abnormal beats are sources of error in QT interval measurements. To avoid this problem we only select three beats in each set of five measured beats. We reject the highest and the lowest QT intervals in this five-beat set. Also we reject those whose QT value is higher or lower than 15 per cent current average.

Following this procedure we plot QT, QT_c, QTP, QTP_c and RR measurements obtained from 24-hour Holter ECG signal recording. The percentage distribution of measurements is also presented as explained below.

3 Validation and results

To evaluate the performance we compare automatic and manual measurements. We have taken a set of n beats at the beginning of 18 tapes, and they have been automatically analysed. Graphic recordings of the same tapes are played back from the Holter system on a paper record at a speed of 25 mm s^{-1}, and manual measurements on the same beats are made by two experts ($expert_1$, $expert_2$)

(MARTÍ *et al.*, 1988). Manual precision is usually 10 ms, and we know that this value also depends on the observer. The differences between two observers can have values even higher than 10 ms in some cases (PISANI *et al.*, 1985; AHNVE, 1985).

Table 1 shows our validation results. We present the number of beats n measured in each tape, the mean difference d^* between automatic and manual measurements, or between experts, and the standard deviation of these differences SD* for each patient. SD and d are values after rejection of maximum and minimum in five beats. Note that SD improves from 17·7 to 14·3 ms (*automatic* $-$ *expert*$_1$) and from 17·4 to 14·4 ms (*automatic* $-$ *expert*$_2$) when we reject these beats, and mean error improves from 2·4 to 2·0 ms, and from 0·9 to 0·4 ms respectively. As noted before, the standard deviation between observers is around 10 ms, similar to that reported in the literature.

The standard deviation of the error between the manual and automatic measurements has a value in the range 10–15 ms. We conclude that reproducibility of the QT interval by computer measurements in this way is comparable to human measurement.

Fig. 8 plots various QRS complex patterns in the 18 tapes along with the QT intervals identified by our algorithm. Note that for patients 2, 3, 4, 5, 6 and 12, no Q-wave is present. Fig. 9 also shows results in some especially noisy beats where we can see the performance in these cases with processing signal and definition points.

We have analysed 18 Holter tapes and as an example we present the results obtained from a 24 hour dynamic QT study in a patient with postmyocardial infarction and malignant ventricular arrhythmia. Fig. 10*b* plots QTP and QT trends for this patient over 24 hours; Fig. 10*c* QTP_c and QT_c trends; and Fig. 10*a* the RR trend for this patient in 24 hours. Each point is the average of measured beats in each 2·5 min period. We can see that the correction with Bazett's formula leads to good results, but there is a remainder QT_c and QTP_c dependence with RR interval variations. This had already been demonstrated by recent works (CRITELLI *et al.*, 1982; SADEH *et al.*, 1987) where discrepancies from Bazett's formula are shown and other correction expressions are based on

$$QT = c(RR)^b \qquad (7)$$

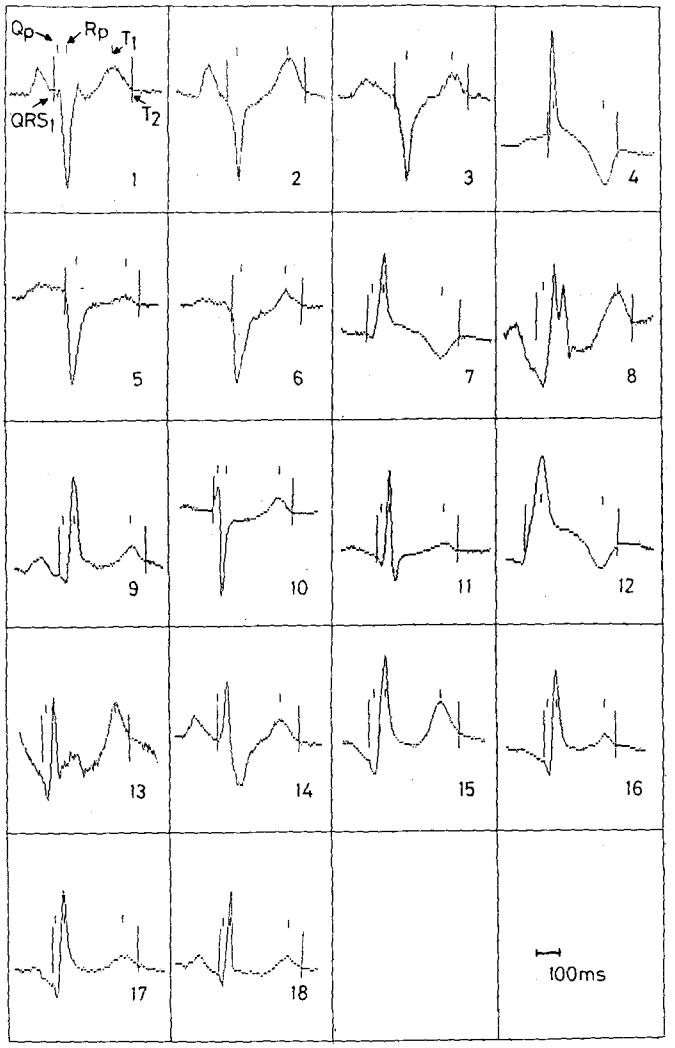

Fig. 8 *Patterns of one beat for each of the 18 tapes used in validation. Long lines show the Q wave beginning QRS_1 and T-wave end T_2 points on these beats as defined by the algorithm; and short lines show Q, R and T peak positions, in this order, when all are present. When there are just two, no Q-wave presence is detected, and R and T-wave peak positions are indicated*

Table 1 Validation results with two manual measurements and between observers on 18 Holter tapes, where n is the number of beats measured on each tape, d is the mean difference between automatic and manual QT interval measurements, and SD* is the standard deviation. d and SD are values after rejection of maximum and minimum QT values in each five-beat set. Units for d, SD, d* and SD* are ms*

		Automatic $-$ *expert*$_1$				*Automatic* $-$ *expert*$_2$				*expert*$_1$ $-$ *expert*$_2$	
Tape	n	d^*	d	SD*	SD	d^*	d	SD*	SD	d^*	SD*
1	34	4·3	2·4	33·9	16·9	7·0	−0·8	36·0	12·6	3·6	12·6
2	42	3·5	3·0	15·1	12·0	1·7	−0·1	11·5	9·8	−0·3	14·7
3	26	−5·9	−8·5	21·0	19·5	−7·7	−7·4	18·8	20·9	2·7	18·5
4	19	−2·3	−2·8	7·7	7·3	−7·2	−7·5	7·3	8·1	4·7	6·8
5	38	4·5	3·2	10·3	8·6	4·5	3·2	10·3	8·6	1·9	10·2
6	49	−21·0	−20·0	10·4	9·0	−22	−21·0	14·4	15·4	0·0	10·7
7	39	−7·2	−10·0	20·4	15·0	−26	−28·0	23·7	17·4	19·2	14·4
8	41	1·0	2·4	13·1	13·3	−1·1	−1·2	14·6	14·5	2·1	14·1
9	29	16·5	16·8	18·7	19·3	16·7	16·5	16·9	17·7	−1·0	5·5
10	39	−8·8	−8·5	13·1	12·4	−7·1	−7·3	14·1	14·9	−1·3	7·6
11	42	9·5	9·1	14·0	11·6	6·8	6·3	11·0	7·5	2·6	7·9
12	45	−17·0	−16·0	16·7	14·6	−18	−15·0	19·1	16·9	0·9	8·4
13	36	8·8	9·4	17·8	15·2	9·4	11·4	19·0	17·5	−0·6	5·7
14	34	7·7	10·9	17·0	14·8	12·3	14·6	17·7	15·7	−4·4	7·3
15	37	8·2	5·1	44·7	22·1	6·1	5·8	39·8	21·9	2·2	15·4
16	35	11·7	11·7	16·0	16·0	9·7	8·5	12·5	11·5	1·7	12·8
17	40	19·6	17·9	13·2	12·9	21·9	21·6	12·3	11·9	−0·2	6·5
18	35	9·5	9·3	15·9	17·5	9·9	8·4	14·8	16·7	−0·3	5·0
Mean	37	2·4	2·0	17·7	14·3	0·9	0·4	17·4	14·4	1·9	10·2

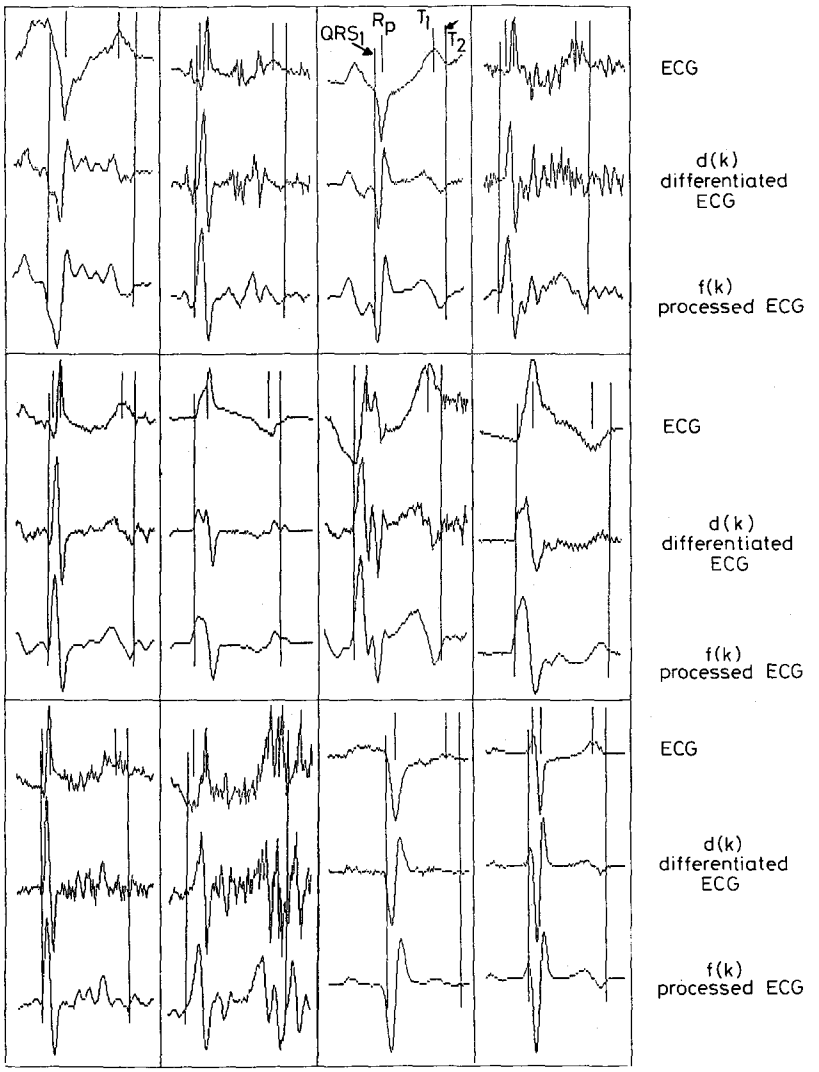

Fig. 9 *Patterns of 12 especially noisy beats, with differentiated and low-pass filtered signals where we can see definition points on every processed signal. The long lines are the QRS onset QRS_1 and T-wave end T_2 points, and the short lines show the Q or R-positions Q_p or R_p and T-wave peak T_1*

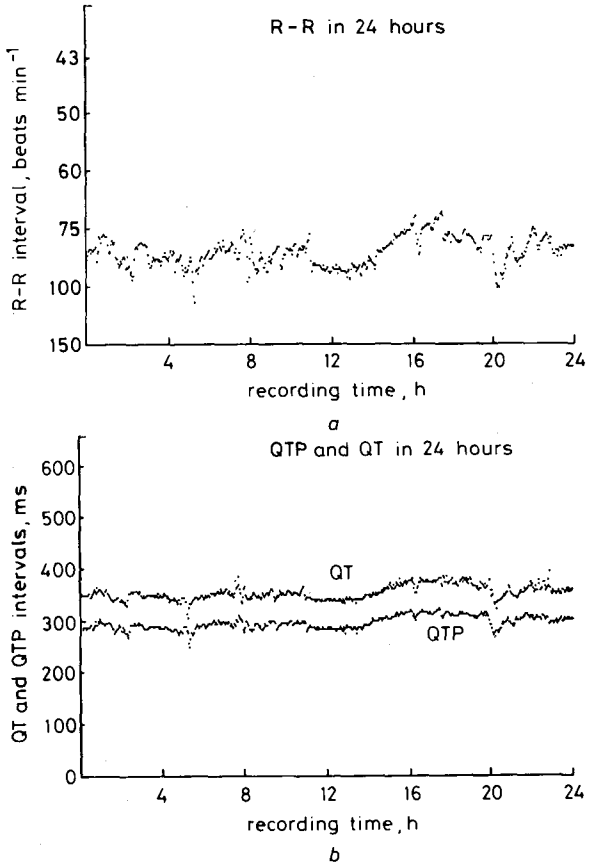

Fig. 10 *Dynamic results obtained from a 24 hour Holter tape. (a) R–R interval translated to beats min^{-1}; (b) QT and QTP intervals in ms; (c) QT_c and QTP_c intervals in ms $s^{-1/2}$. Each point on the graph is the average of measured interval values in periods of 2·5 min*

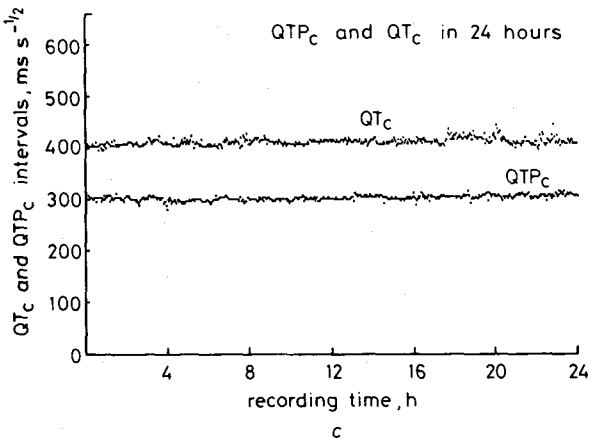

Table 2 Results from a patient. QT, QT_c, QTP, QTP_c and R–R intervals are plotted as percentage of beats in 20 ms intervals for QT values, and intervals of 100 ms for RR values. Results are rounded to nearest whole integer numbers

Interval, ms	*QT*, beats per cent	*QTP*, beats per cent	QT_c, beats per cent	QTP_c, beats per cent	Interval, ms	*RR*, per cent
240–260	—	1	—	—	400– 500	—
260–280	—	21	—	—	500– 600	—
280–300	—	53	—	3	600– 700	—
300–320	—	23	—	38	700– 800	15
320–340	—	2	—	48	800– 900	49
340–360	4	—	—	10	900–1000	24
360–380	32	—	2	1	1000–1100	9
380–400	38	—	26	—	1100–1200	3
400–420	23	—	55	—		
420–440	3	—	15	—		
440–460	—	—	2	—		

Bazett's formula uses $b = \frac{1}{2}$ and SADEH *et al.* (1987) proposed $b = 0{\cdot}13$. These discrepancies suggest future investigation in a higher number of patients, and dependency on pathology, age etc.

Data are also analysed by classifying the measurements obtained in intervals of 20 ms for *QT*, QT_c, *QTP* and QTP_c, and in intervals of 100 ms for *RR* interval. Table 2 presents the percentage of beats in each interval.

4 Discussion and conclusions

A new algorithm is presented for QT interval measurement. Its accuracy is comparable with results of other QT algorithms (ALGRA *et al.*, 1987; PISANI *et al.*, 1985) and to manual measurement, but it has a better immunity to baseline interferences when the baseline differs from a flat line after T-end, a situation quite common in Holter ECG recordings. Other algorithms for QRS onset (Q-beginning) involve a significantly higher amount of calculation for a comparable performance (NYGÅRDS and SÖRNMO, 1983).

At present this system is implemented in 'turbo Pascal' language and runs on a PC compatible, taking about 90 min processing time in a Compaq III computer for 24 hour recorded ECG. No ectopic beat rejection is implemented in the QRS detector, thus the subsequent selection is supposed to remove these abnormal beats. Problems can be found in ventricular tachycardia or ventricular fibrillation; in these cases the algorithm will give nonsense values because no QT interval is defined. Further work to detect and remove this kind of interference is required.

Also, in sequences with very low signal-to-noise ratios wrong values can result. Moreover, if these sequences are only of one or a small number of beats, the problem is minimised by rejection criteria. Now the problem is only important in recordings where there is an electrode problem or continuous interference occurs.

The availability of 24 hour ECG signal processing, to make use of the QT interval as a marker of MVA in PMIP, is presented. The relationship and dependence of QT and QT_c in patients with different pathologies suggests further investigation to show the real value of these parameters as predictors of sudden death and other heart diseases (MARTÍ *et al.*, 1988); this is the reason for the presentation as a percentage of beats in some defined intervals. The interpretation of the QT_c interval to quantify prognosis in PMIP should take into account at least the inaccuracy of measurements. A study of the relationship between QTP_c and QT_c will be interesting, because if both give the same information QTP measurement is more accurate than QT.

Acknowledgments—This work was supported by a fellowship (to PL) from the 'CIRIT' Generalitat de Catalunya, Spain, and grants NS24282 and HL (to NVT) from the National Institute of Health, USA, and 1240/84 (to PC) from CAICYT Spain and Fundacion Roviralta (ACARD) Spain.

References

AHNVE, S., LUNDMAN, T. and SHOALEH-VAR, M. (1978) The relationship between QT interval and primary ventricular fibrillation in acute myocardial infarction. *Acta Med. Scand.*, **204**, 17–19.

AHNVE, S. (1985) Errors in visual determination of corrected QT (QTc) interval during acute myocardial infarction. *J. Am. Coll. Cardiol.*, **5**, 699–702.

ALGRA, A., LE BRUN, H. and ZEELENBERG, C. (1987) An algorithm for computer measurement of QT intervals in the 24 hour ECG. In *Computers in Cardiology*. IEEE Computer Society Press, 117–119.

BAZETT, H. C. (1920) An analysis of the time relation of electrocardiograms. *Heart*, **7**, 353–370.

CRITELLI, G., MARCIANO, F., MAZZARELLA, M. and MIGAUX, M. L. (1982) QT interval measurements of long-term ECG recordings. Application to an automatic Holter analysis system. In *Computers in Cardiology*, IEEE Computer Society Press, 481–480.

LYNN, P. A. (1977) Online digital filters for biological signals: some fast designs for a small computer. *Med. & Biol. Eng. & Comput.*, **15**, 534–540.

MARTÍ, V., BAYÉS DE LUNA, A., ARRIOLA, J., SONGA, V., GUINDO, J., DOMINGUEZ DE LAS ROZAS, J., MARRUGAT, J., SANZ, F., THAKOR, N., MIN, Y., CAMINAL, P. and LAGUNA, P. (1988) Value of dynamic QTc in arrhythmology. Proc. 8th. Int. Congr. The New Frontiers of Arrythmias, Marilleva, Italy, 683–691.

NYGÅRDS, M.-E. and SÖRNMO, L. (1983) Delineation of the QRS complex using the envelope of the e.c.g. *Med. & Biol. Eng. & Comput.*, **21**, 538–547.

PAN, J. and TOMPKINS, W. J. (1985) A real time QRS detection algorithm. *IEEE Trans.*, **BME-32**, 230–236.

PISANI, E., PELLEGRINI, E., ANSUINI, G., DI NOTO, G., RIMATORI, C. and RUSSO, P. (1985) Performance evaluation of algorithms for QT interval measurements in ambulatory ECG recording. In *Computers in Cardiology*, IEEE Computer Society Press, 459–462.

PUDDU, P. E., JOUVE, R., TORRESANI, J. and JOUVE, A. (1981) QT interval and primary ventricular fibrillation in acute myocardial infarction. *Am. Heart J.*, **101**, 118–119.

PUDDU, P. E. and BOURASSA, M. G. (1986) Prediction of sudden death from QTc interval prolongation in patients with chronic ischemic disease. *J. Electrocardiol.*, **19**, 203–212.

SADEH, D., SHANNON, D. C., ABBOUD, S., AKSELROD, S. and COHEN, R. J. (1987) A new technique to determine the correlation between the QT interval and heart rate for control and sids babies. In *Computers in Cardiology*, IEEE Computer Society Press, 125–127.

SCHWARTZ, P. J. and WOLF, S. (1978) QT interval prolongation as predictor of sudden death in patients with myocardial infarction. *Circ.*, **57**, 1074–1077.

TAYLOR, G. J., CRAMPTON, R. S., GIBSON, R. S., STEBBINS, P. T., WALDMAN, M. T. G. and BELLER, G. A. (1981) Prolonged QT interval at onset of acute myocardial infarction in predicting early phase ventricular tachicardia. *Am. Heart J.*, **102**, 16–24.